Int. J. Solids Structures, 1970, Vol. 6, pp. 259 to 275. Pergamon Press. Printed in Great Britain

A NEW METHOD OF REINFORCING A HOLE EFFECTING LARGE WEIGHT SAVINGS*

S. K. DHIR† and J. S. BROCK‡

Naval Ship Research and Development Center,
Washington D.C. 20007

Abstract—A new method of reinforcing a hole in a flat plate under uniaxial tension is proposed in which the reinforcing material is present on the boundary of the hole only in the regions containing high stresses. Since the reinforcement is discontinuous, its amount, which varies along the arcs of the hole, is represented by a Fourier series in the analysis of the stresses. The stresses are determined by the use of two complex potential functions in series form. The series are truncated at the point whereafter any additional terms do not produce any significant change in the magnitude of the stresses. Numerical values are given for the case of a circular hole with various types of reinforcements. Finally, it is shown that this type of reinforcement can effect approximately 60 to 70 per cent savings in weight along with a 30 to 35 per cent savings in the welding and about 10 per cent reduction in the maximum stress as compared to the conventional all around reinforcement.

NOTATION

A	Area of cross section of the reinforcing ring
a_n, b_n	Constants in potential functions
C	Constant
D	Maximum value of $F(\theta)$
h	Height of reinforcement
L_n, M_n	Constants in the Fourier Series
F_0, R_0, S_0	Forces on reinforcement element
R	Radius of circular opening
R_e	Ratio of area replaced to area removed (A/Rt)
T_0	Applied tensile stress at infinity
t	Thickness of plate
z	Complex plane ($x+iy$)
α, β	Curvilinear coordinates
β_0, γ	Angular dimensions of reinforcement
ζ	Complex plane ($e^{\alpha+i\beta}$)
θ	Polar Angle
ν	Poisson's ratio
σ	Boundary value of ζ at $\alpha = 0$
$\sigma_\alpha, \sigma_\beta, \tau_{\alpha\beta}$	Curvilinear stresses
$ds, d\theta$	Linear and angular increments
$F(\theta)$	Reinforcement function
$\varphi(z), \psi(z)$	Potential functions in z-plane
$\varphi(\zeta), \psi(\zeta)$	Potential functions in ζ-plane

* The opinions expressed are those of the authors alone and should not be construed to reflect the official views of the Navy Department or the Navy Service at large.

† Physicist.

‡ Structural Engineer.

INTRODUCTION

THE use of reinforcements at the boundaries of various kinds of openings is common practice in ship and aircraft construction. Beginning with the Kirsch [1] solution of a circular hole in an infinite plate under uniaxial tension, many other papers [2–7] are documented in the literature which deal with the boundary value problem of the reinforcement of a circular opening in a flat plate under various loading conditions. In the above investigations the reinforcement of the circular opening is accomplished by means of a continuous ring, doubler plate or combination ring and doubler plate which extend uniformly around the periphery of the opening. This constitutes indiscriminate use of reinforcing material since a substantial proportion of this material is distributed in regions of low stress. The reinforcing material in the low-stress region is effectively wasted. Such ineffective use of material is a disadvantage and a severe limitation for an optimum design, especially for weight critical structures such as high speed destroyers, surface effect ships, deep submergence vehicles, etc.

In view of the above it appears logical to reinforce the opening only in the regions of high stress rather than providing conventional all around reinforcement. An obvious advantage of this new type of reinforcement is realized in large weight savings.

The principal objective of this paper is, therefore, to determine the stresses around any general shaped opening in a large flat plate under uniaxial load when the opening is reinforced only in certain discrete regions, viz. the highly stressed regions.

The method of solution is based on the approach developed by Muskhelishvili [8] for solving the plane elasticity problems and the following assumptions:

1. The plate is thin compared to the other dimensions and extends to infinity in both x- and y- directions.
2. The plate material is elastic, isotropic and homogeneous.
3. The reinforcing material is the same as that of the parent plate and is concentrated on the boundary of the opening (compact reinforcement).
4. The reinforcement can be subject to hoop stresses only and has no bending stiffness.

The first two are the usual assumptions for a generalized plane stress system within the theory of elasticity. The third assumption is clearly justified since the opening is usually large compared to the reinforcement. The last assumption is based on the findings of References [5] and [6], which suggest that the effect of bending stiffness on the overall stress field is of second order. The effect of nonuniform stiffness of reinforcement is assumed to be small as in Reference [9].

The cross sectional area of the reinforcement at any specific point on the boundary of the opening is assumed to be a function of the angular coordinate and can have any desired distribution. The method developed in the present paper is general so that it is applicable to an opening of any shape. As an illustration of the method the case of a circular opening is considered in detail. The numerical values for the boundary stresses are given for a number of reinforcement distributions. Finally, it is shown that, by this method, not only large savings in the weight of reinforcement but also substantial savings in the amount of welding and a simultaneous reduction in the magnitude of maximum stress can be realized.

BOUNDARY CONDITIONS

Figure 1 shows an opening of general continuous shape which is reinforced in the region 1 2 3. There is no reinforcing material present in 3 1. The forces acting on an element, ds, of reinforcement are shown in Fig. 2. If this boundary is to be in elastic equilibrium the following equation must hold true.

$$\begin{aligned} \frac{\partial F_0}{\partial s}\,\mathrm{d}s + S_0\,\mathrm{d}s &= 0 \\ R_0\,\mathrm{d}s - F_0\,\mathrm{d}\beta &= 0 \\ R_0 &= \sigma_\alpha t \\ S_0 &= \tau_{\alpha\beta} t. \end{aligned} \tag{1}$$

Furthermore, the circumferential strain in the reinforcement must be the same as that in the adjoining plate boundary, therefore

$$F_0 = A(\sigma_\beta - \nu\sigma_\alpha) \tag{2}$$

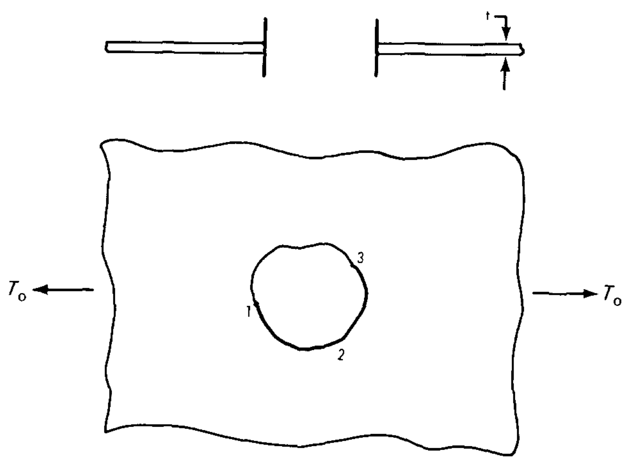

FIG. 1. Reinforced hole.

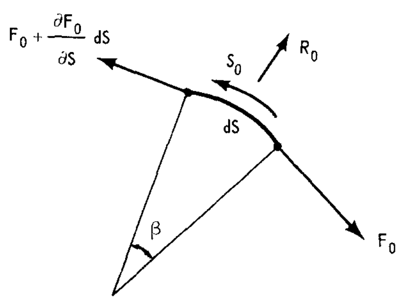

FIG. 2. Forces on boundary.

where A is the cross-sectional area of the reinforcement.

From equations (1) and (2) it follows that

$$\sigma_\alpha = \frac{\frac{A}{t}}{\frac{ds}{d\beta}+\nu\frac{A}{t}}\sigma_\beta$$
$$\tau_{\alpha\beta} = -\frac{\partial}{\partial s}\left(\frac{\frac{A}{t}\sigma_\beta\frac{ds}{d\beta}}{\frac{ds}{d\beta}+\nu\frac{A}{t}}\right) \tag{3}$$

with

$$F(\vartheta) = \frac{\frac{A}{t}}{\frac{ds}{d\beta}+\nu\frac{A}{t}} \tag{4}$$

the boundary conditions represented by equations (3) can be conveniently written as

$$\sigma_\alpha = F(\vartheta)\sigma_\beta$$
$$\tau_{\alpha\beta} = -\frac{\partial}{\partial s}\left[\frac{ds}{d\beta}F(\vartheta)\sigma_\beta\right]. \tag{3a}$$

The function $F(\vartheta)$ will be referred to as the reinforcement function. The solution of the problem is thus contained in the analysis of the equations (3a).

REINFORCEMENT

The reinforcing function $F(\vartheta)$ can be represented as a complex Fourier series such that

$$F(\vartheta) = \sum_{n=0}^{\infty}\left(L_n\sigma^n+\frac{M_n}{\sigma^n}\right) \tag{5}$$

where σ is the boundary value of the function $\zeta = e^{\alpha+i\beta}$ for $\alpha = 0$ and L_n, M_n are the constants, possibly complex, in the expansion. It may be pointed out that a suitable choice of the constants L_n, M_n will permit reinforcements of any size and distribution within the region 0 to 2π. The above series, equation (5), can be suitably truncated to obtain any desired degree of accuracy for a particular desired distribution of the reinforcing material.

DETERMINATION OF STRESSES

The stress components in a cartesian plane defined by $z = x+iy$ are given by

$$\sigma_x+\sigma_y = 2[\varphi'(z)+\overline{\varphi'(z)}]$$
$$\sigma_y-\sigma_x+2i\tau_{xy} = 2[\bar{z}\varphi''(z)+\psi'(z)] \tag{6}$$

where a prime (′) indicates differentiation with respect to the argument of the function and a bar (–) is the conjugate complex.

In order to solve problems for general shapes of the boundary, use may be made of conformal mapping of the boundaries onto the unit circle, such that

$$z = z(\zeta). \tag{7}$$

With the application of equation (7) it is simple to show that the following equations hold good at the boundary $\zeta = \sigma$

$$\begin{aligned}\sigma_\beta &= \frac{\varphi'(\sigma)}{z'(\sigma)}+\frac{\sigma^2}{2\overline{z'(\sigma)}}\left[\overline{z(\sigma)}\left(\frac{\varphi'(\sigma)}{z'(\sigma)}\right)'+\psi'(\sigma)\right]\quad \frac{\overline{\varphi'(\sigma)}}{\overline{z'(\sigma)}}+\frac{1}{2\sigma^2 z'(\sigma)}\left[z(\sigma)\overline{\left(\frac{\varphi'(\sigma)}{z'(\sigma)}\right)'}+\overline{\psi'(\sigma)}\right]\\ \sigma_\alpha - i\tau_{\alpha\beta} &= \frac{\varphi'(\sigma)}{z'(\sigma)}+\frac{\overline{\varphi'(\sigma)}}{\overline{z'(\sigma)}}-\frac{\sigma^2}{2\overline{z'(\sigma)}}\left[\overline{z(\sigma)}\left(\frac{\varphi'(\sigma)}{z'(\sigma)}\right)'+\psi'(\sigma)\right].\end{aligned} \tag{8}$$

For a particular coordinate system defined by equation (7) it can be shown that

$$\frac{\partial}{\partial s} = \frac{1}{(z'\bar{z}')^{\frac{1}{2}}}\frac{\partial}{\partial\beta}. \tag{9}$$

Equations 3(a) permit the representation of σ_α and $\tau_{\alpha\beta}$ in terms of the stress σ_β, the radius of curvature of the actual opening and the reinforcement function $F(\vartheta)$. The second of equations (8) is a representation of the combination stresses $\sigma_\alpha - i\tau_{\alpha\beta}$ exclusively in terms of the boundary values of the potential functions $\varphi(\zeta)$ and $\psi(\zeta)$ and the mapping function $z(\zeta)$. Therefore we have the following equivalence at $\zeta = \sigma$

$$\begin{aligned}&\frac{\varphi'(\sigma)}{z'(\sigma)}+\frac{\overline{\varphi'(\sigma)}}{\overline{z'(\sigma)}}-\frac{\sigma^2}{2\overline{z'(\sigma)}}\left[\overline{z(\sigma)}\left(\frac{\varphi'(\sigma)}{z'(\sigma)}\right)'+\psi'(\sigma)\right]\\ &\quad = F(\vartheta)+\frac{i}{(z'\bar{z}')^{\frac{1}{2}}}\frac{\partial}{\partial\beta}\left[\frac{\mathrm{d}s}{\mathrm{d}\beta}F(\vartheta)\right]\quad \sigma_\beta+\frac{\mathrm{d}s}{\mathrm{d}\beta}F(\vartheta)\frac{i}{(z'\bar{z}')^{\frac{1}{2}}}\frac{\partial}{\partial\beta}\sigma_\beta\end{aligned} \tag{10}$$

where σ_β is given by first of equations (8).

Since the functions $\varphi(\zeta)$ and $\psi(\zeta)$, whose boundary values at $\zeta = \sigma$ are $\varphi(\sigma)$ and $\psi(\sigma)$, are analytic on the outside of the unit circle in the ζ-plane, the two functions $\varphi(\zeta)$ and $\psi(\zeta)$ can be conveniently represented in the following form

$$\begin{aligned}\varphi(\zeta) &= \frac{T_0 C}{4}\left[\zeta+\sum_{1}^{\infty}\frac{a_n}{\zeta^n}\right]\\ \psi(\zeta) &= \frac{T_0 C}{4}\left[-2\,\mathrm{e}^{-2i\alpha_0}\zeta+\sum_{0}^{\infty}\frac{b_n}{\zeta^n}\right]\end{aligned} \tag{11}$$

where T_0 is the uniform tension at infinity at an angle α_0 to the x-axis and C is a constant. The solution of the problem is now reduced to the determination of the complex constants a_n and b_n which can be easily realized by using one of the methods due to Muskhelishvili. After the constants a_n and b_n have been determined equations (8) can be used to obtain the individual stress components.

REINFORCED CIRCULAR HOLE

As shown in Figs. 3a and 3b the reinforcement function $F(\vartheta)$ has the value zero from 0 to γ and increases linearly to a maximum value D at $\pi/2-\beta_0$ whereafter it remains constant up to $\pi/2$. From a practical standpoint the reinforcement function $F(\vartheta)$ has been chosen to have a double symmetry. For the present case of a circular hole equation (4) will reduce to

$$F(\vartheta) = \frac{\dfrac{A}{Rt}}{1+\nu\dfrac{A}{Rt}} \tag{12}$$

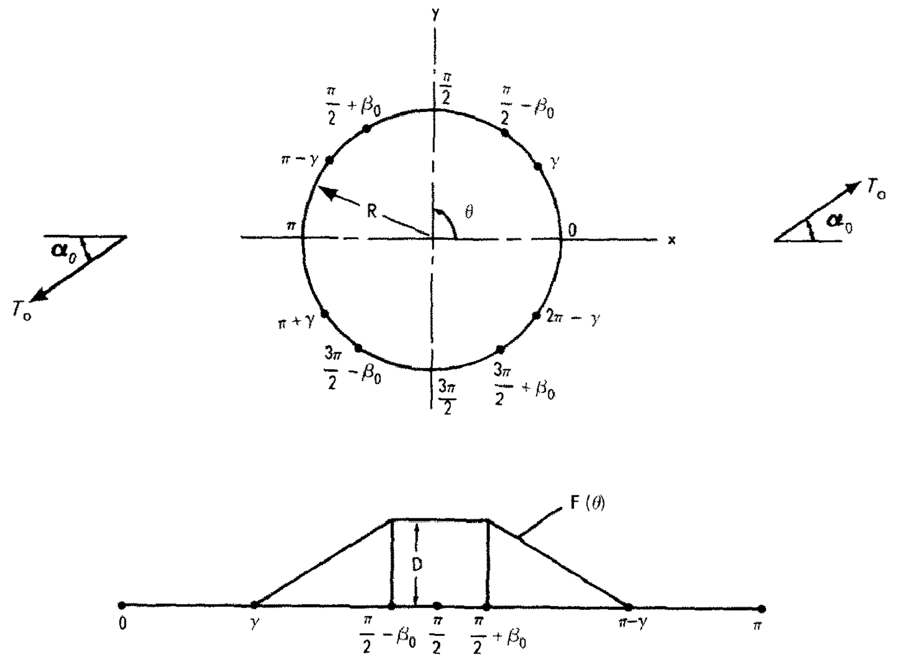

FIG. 3. Reinforced circular hole.

since $ds/d\beta$ is the radius of curvature R of the circular hole. The dimensionless quantity A/Rt now becomes the ratio of the area of cross section, A, of the reinforcement (area replaced) to the cross sectional area, Rt, removed due to the hole. Equation (12) can be rearranged as

$$R_e = \frac{A}{Rt} = \frac{F(\vartheta)}{1-\nu F(\vartheta)}. \tag{13}$$

Equation (13) clearly shows that the ratio R_e of area replaced to area removed remains constant for a constant value of $F(\vartheta)$. However, if $F(\vartheta)$ is linearly varying then R_e is non-linear; the departures from linearity are small and can be computed for individual cases.

The function $F(\vartheta)$ as shown in Fig. 3 can be represented by equation (5) if $M_n = L_n$ (symmetry requirement)

$$
\begin{aligned}
L_0 &= \frac{\pi+2(\beta_0-\gamma)}{4\pi} \\
L_{2n} &= \frac{(-1)^n \cos 2n\beta_0 - \cos 2n\gamma}{\pi n^2[\pi-2(\beta_0+\gamma)]}, n \geq 1 \\
L_{2n-1} &= 0, n \geq 1.
\end{aligned} \tag{14}
$$

Some reinforcements, having distributions other than shown in Fig. 3 and, which are of academic interest are when the amount of reinforcing material varies according to a cosine distribution. For example if $L_0 = -L_2$ has a non-zero value K and all the other L_n are zero, then

$$F(\vartheta) = K(1-\cos 2\vartheta). \tag{15}$$

On the other hand if

$$
\begin{aligned}
L_0 &= L_2 = \frac{K}{4} \\
L_{2n} &= 0, \qquad n \geq 2 \\
L_{2n-1} &= (-1)^{n+1} \frac{4K}{\pi(2n-3)(2n-1)(2n+1)}, n \geq 1
\end{aligned} \tag{16}
$$

then $F(\vartheta)$ will be zero from 0 to $\pi/4$, vary according to $K(1+\cos 4\vartheta)$ from $\pi/4$ to $(3\pi/4)$ and remain zero from $(3\pi/4)$ to π. It may be pointed out that all the above reinforcement distributions have a frequency 2 with a period π within the region 0 to 2π.

The outside of a circular hole of radius R can be mapped onto the outside of unit circle in the ζ-plane by

$$z = R\zeta. \tag{17}$$

The value of the constant C is equations (11), for this case, becomes R. Equation (10) which is the boundary condition for any general shaped hole, in the present case, reduces to

$$
\begin{aligned}
&2+2e^{-2i\alpha_0}\sigma^2 - \sum_0^\infty \frac{(n+1)(n-1)a_{n-1}-(n+1)b_{n+1}}{\sigma^n} - \sum_0^\infty (n-1)\bar{a}_{n-1}\sigma^n \\
&= \left\{\sum_0^\infty \left[K_n\sigma^n + \frac{\bar{K}_n}{\sigma^n}\right]\right\}\left\{1+\frac{1}{2}\sum_0^\infty \frac{(n-1)(n-2)a_{n-1}-(n+1)b_{n+1}}{\sigma^n} - \frac{e^{2i\alpha_0}}{\sigma^2}\right. \\
&\quad \left. +1-e^{-2i\alpha_0}\sigma^2 + \frac{1}{2}\sum_0^\infty [(n-1)(n-2)\bar{a}_{n-1}-(n+1)\bar{b}_{n+1}]\sigma^n\right\} \\
&\quad +\left\{\sum_0^\infty L_n\left(\sigma^n+\frac{1}{\sigma^n}\right)\right\}\left\{2\,e^{-2i\alpha_0}\sigma^2 + \frac{1}{2}\sum_0^\infty \frac{n(n-1)(n-2)a_{n-1}-n(n+1)b_{n+1}}{\sigma^n}\right. \\
&\quad \left. -\frac{2\,e^{2i\alpha_0}}{\sigma^2} - \frac{1}{2}\sum_0^\infty [n(n-1)(n-2)\bar{a}_{n-1}-n(n+1)\bar{b}_{n+1}]\right\}
\end{aligned} \tag{18}
$$

where

$$K_n = (1-n)L_n$$
$$\bar{K}_n = (1+n)L_n$$

Either by successive integration of equation (18) around the unit circle or by equating to zero the sum of the coefficients of equal powers of σ, we obtain

$$
\begin{aligned}
&b_1 + L_0(b_1+\bar{b}_1) + \sum_{m=1}^{\infty} (2m-1)L_m(a_{m-1}+\bar{a}_{m-1}) = 4L_0 + 2L_2(e^{2i\alpha_0}+e^{-2i\alpha_0}) - 2 \\
&\bar{a}_{n-1} + \sum_{m=1}^{\infty} (2m-1)(L_{m-n}\bar{a}_{m-1} + L_{m+n}a_{m-1}) + \sum_{m=1}^{n} (2m-1)L_{n-m}\bar{a}_{m-1} \\
&\quad + \frac{L_n}{2}(b_1+\bar{b}_1) = 2(\delta_{n,2}+L_{n-2}+L_{2-n})e^{-2i\alpha_0} + 2L_{2+n}e^{2i\alpha_0} + 2L_n; \qquad n \geq 1 \\
&b_{n+1} = na_{n-1} - \delta_{n,2}\,2\,e^{2i\alpha_0}; \qquad n \geq 1
\end{aligned}
\tag{19}
$$

where $\delta_{m,n}$ is the Kronecker delta.

Equations (19) can now be broken into two sets by separating the real and imaginary parts of the system. It can be easily shown that if $\alpha_0 = 0$ the imaginary part of the system vanishes and the real system becomes

$$
\begin{aligned}
&(1+2L_0)b_1 + \sum_{m=1}^{\infty} 2(2m-1)L_m a_{m-1} = 4L_0 + 4L_2 - 2 \\
&\sum_{m=1}^{\infty} (2m-1)\left[L_{m-n} + L_{m+n} + L_{n-m} + \frac{\delta_{m,n}}{2m-1}\right] a_{m-1} + L_n b_1 \\
&\quad = 2(\delta_{n,2} + L_{n-2} + L_{2-n} + L_{2+n}) + 2L_n; \qquad n \geq 1 \\
&b_{n+1} = na_{n-1} - 2\delta_{n,2}. \qquad n \geq 1
\end{aligned}
\tag{20}
$$

The above infinite system of linear algebraic simultaneous equations is very intricate Therefore it was necessary to truncate the above system such that it could be programmed and solved on a digital computer. The system was truncated at a point where acceptable convergence was obtained and any further additional terms did not produce any significant change in the magnitude of the stresses. Stresses with absolute magnitudes greater than 0·1 are computed to an accuracy of at least 0·3 of 1 per cent for $T_0 = 1$. These stresses are therefore numerically equal to the stress concentration factors.

RESULTS AND DISCUSSION

Although a large number of variations are possible in the distribution of the reinforcing material, only those which appeared important from a practical standpoint were studied. These cases are enumerated in Table 1 together with the tangential stress at $\pi/2$ and the local maximum tangential stress. The last column of Table 1 shows the percentage of the weight of reinforcement saved when compared to the all around reinforcement of case 14 with the exception of case 7 where the comparison is based on an all around $R_c = 1{\cdot}0$. Case 14 of all around reinforcement checks with the results of reference 6

TABLE 1. SUMMARY OF RESULTS

No.	R_e	β_0 Deg.	γ Deg.	σ_β at $\vartheta = \pi/2$	Local maximum σ_β and remarks	Weight* saving %
1	0·4	0	0	1·562	1·659(80°)	50
2	0·4	0	30	1·467	1·672(70°)	67
3	0·4	0	45	1·356	2·588(45°)	75
4	0·4	5	35	1·489	1·623(65°)	67
5	0·4	7	37	1·489	1·602(65°)	67
6	0·4	10	30	1·556	1·548(70°)	61
7	1·0	10	30	1·053	1·830(30°)	61
8	0·4	10	35	1·535	1·584(35°)	64
9	0·4	15	30	1·590	1·465(65°)	58
10	0·4	15	35	1·571	1·696(35°)	61
11	0·4	0	0	1·612	Smooth cosine	50
12	0·4	0	45	1·359	2·53(50°), Cosine	75
13	0·4	45	44	1·655	3·894(40°)	49
14	0·4	90	0	1·702	All around	--
15	0·4	5·73	26·97	1·532	1·606(71°)	62
16	0·4	9·55	32·7	1·538	1·558(69°)	63

* The numbers in this column refer to the percentage of the weight saved compared to the all around reinforcement.

The boundary stresses σ_α, σ_β and $\tau_{\alpha\beta}$ were computed at intervals of 5 degrees for the cases listed in Table 1. The sample values of σ_α, σ_β and $\tau_{\alpha\beta}$ are given in Table 2 for case 16. The last column in Table 2 shows the values of the reinforcing function $F(\vartheta)$. In accordance with one of the boundary conditions given by the first of equations (3a), $F(\vartheta)$ when multiplied with σ_β should give σ_α at the boundary of the hole. This served as a good check on the computations and is evidenced in Table 2.

TABLE 2. SAMPLE VALUES OF STRESS FOR CASE 16 OF TABLE 1

ϑ	σ_α	σ_β	$\tau_{\alpha\beta}$	$F(\vartheta)$
0	0	−0·8983	0	0
5	0	−0·8678	0	0
10	0	−0.7702	0	0
15	0	−0·5895	0	0
20	0	−0·3036	0	0
25	0	0·1159	0	0
30	0	0·7842	0	0
35	0·0190	1·2746	−0·482	0·0171
40	0·0649	1·2068	−0·5766	0·0546
45	0·1198	1·3055	−0·6670	0·0920
50	0·1812	1·3977	−0·7280	0·1294
55	0·2463	1·4726	−0·7555	0·1668
60	0·3121	1·5261	−0·7476	0·2042
65	0·3755	1·5550	−0·7033	0·2416
70	0·4335	1·5565	−0·6231	0·2790
75	0·4831	1·5296	−0·5071	0·3163
80	0·5210	1·4759	−0·3444	0·354
85	0·5426	1·5198	−0·1598	0·3572
90	0·5496	1·5381	0	0·3571

Figures 4–8 show the distribution of the boundary stress and the reinforcement function $F(\vartheta)$ along the periphery of the opening for most of the cases given in Table 1. In the Fourier series expansion of the reinforcement function $F(\vartheta)$, 95 non-zero terms had to be retained in order to closely approximate the desired shape. However, the discontinuities in the function $F(\vartheta)$ due to sudden changes in the amount of reinforcement were automatically removed because of the truncation. This is clearly indicated in the σ_β-curves which do not approach infinity (theoretical value of the stress at discontinuities) but only show a light stress concentration. A quantitative relationship between this local stress concentration and the degree of smoothing of reinforcement due to truncation can be established by properly analyzing the truncated function $F(\vartheta)$ and correlating it with the computed stress concentration. For reinforcements such as case 13 generous fillet welds should be used to avoid localized stress concentration. In general, the stress σ_β appears to be always negative at $\vartheta = 0$, which is expected since $\vartheta = 0$ coincides with the direction of the load. With increasing value of ϑ, σ_β passes through zero and reaches a local maximum in the vicinity of the beginning of the reinforcement, passes through another local maximum and a local minimum in the neighborhood of the point where $F(\vartheta)$ assumes a constant value and finally σ_β assumes its value at $\vartheta = \pi/2$, which in the conventional types of all around reinforcement happens to be the point of maximum stress.

It is interesting to note that in spite of the smoothness afforded by the cosine distribution of the reinforcement function $F(\vartheta)$ the stress in cases 11 and 12 are not particularly superior or desirable. This can be explained by the fact that a cosine distribution does not represent a streamlined shape and therefore is still subject to stress concentrations, case 12 of Fig. 7.

It appears from Figs. 4 through 8 that the σ_β-stress distribution is quite sensitive to the slope of the function $F(\vartheta)$ between the two points where the reinforcement begins and becomes constant. This behavior has a close relationship with the theory of flank angles in notches and fillets. The local stress concentration at the beginning of the reinforcement is a function of the flank angle formed by $F(\vartheta)$ at that point. This can be observed in Fig. 5 where increasing the amount of reinforcement from $R_e = 0{\cdot}4$ (case 6) to $R_e = 1{\cdot}0$ (case 7) decreased the flank angle and hence the stress concentration was increased. An inspection of Figs. 4 through 7 shows that for the same flank angle the maximum stress concentration occurs for larger values of γ. This is quite obvious since the nominal stress, boundary stress at the point without reinforcement, for a circular opening is larger for larger values of γ. It is, therefore, imperative to properly select the point where to begin the reinforcement. Near optimum conditions can be arrived at by investigating various combinations of R_e, β_0 and γ.

Out of all the cases considered case 16 appears to be the most favorable from a stress point of view. The magnitudes of the parameters β_0 and γ for case 16 were the results of following consideration.

From a designer's standpoint it is more desirable to describe the dimensions of the reinforcement as fractions or multiples of the dimensions of the opening. Figure 9(a) shows a circular opening of radius R symmetrically reinforced on the arcs 2 3 4 5 and 2′ 3′ 4′ 5′. The cross hatched portion 2 3 4 5 4 3 2 of Fig. 9(b) is the development of the reinforcement 2 3 4 5 (neglecting the nonlinearity of R_e) of Fig. 9(a) on a plane. The height h of the reinforcement can be suitably chosen depending on the thickness of the parent plate. The area 1 3 4 6 4 3 1 would be the development of the reinforcement if it were all around the opening. The savings in the weight of the reinforcement can be easily

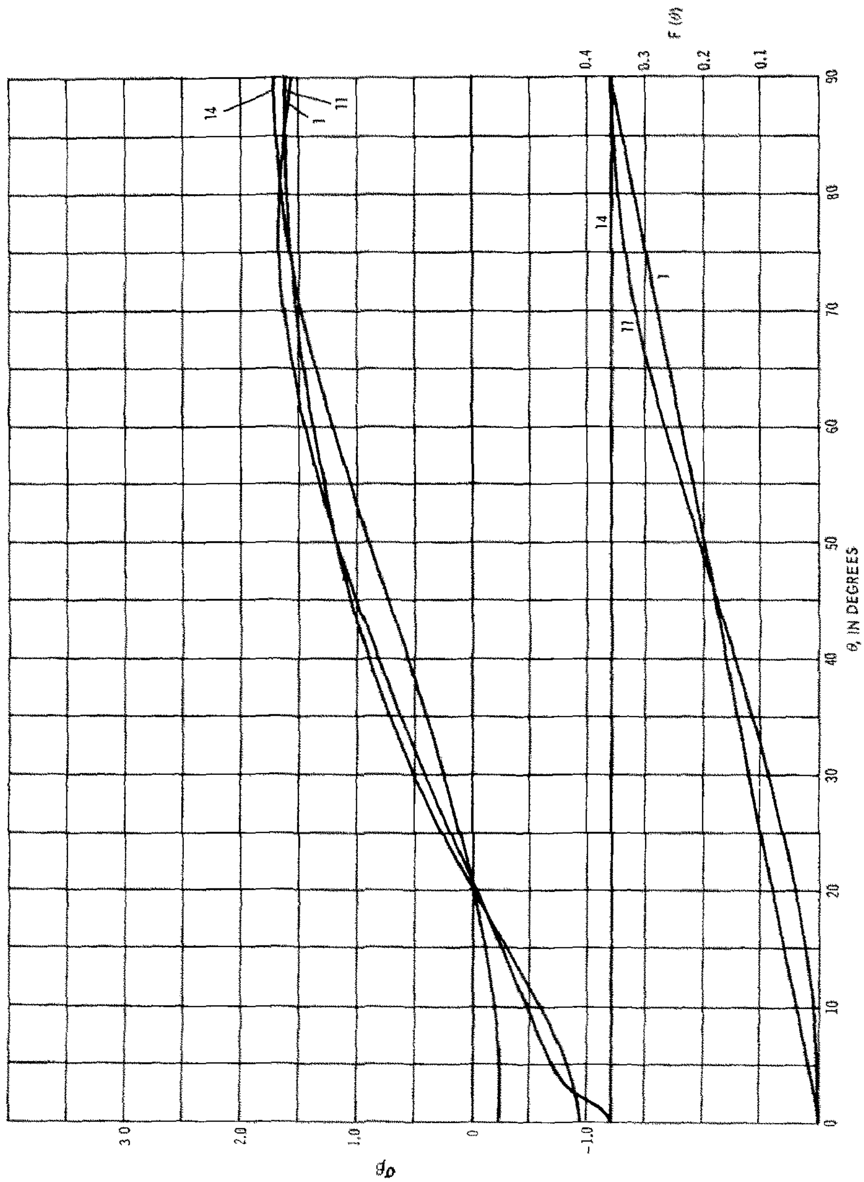

FIG. 4. σ_β and $F(\vartheta)$ as functions of ϑ, case 1, 11 and 14.

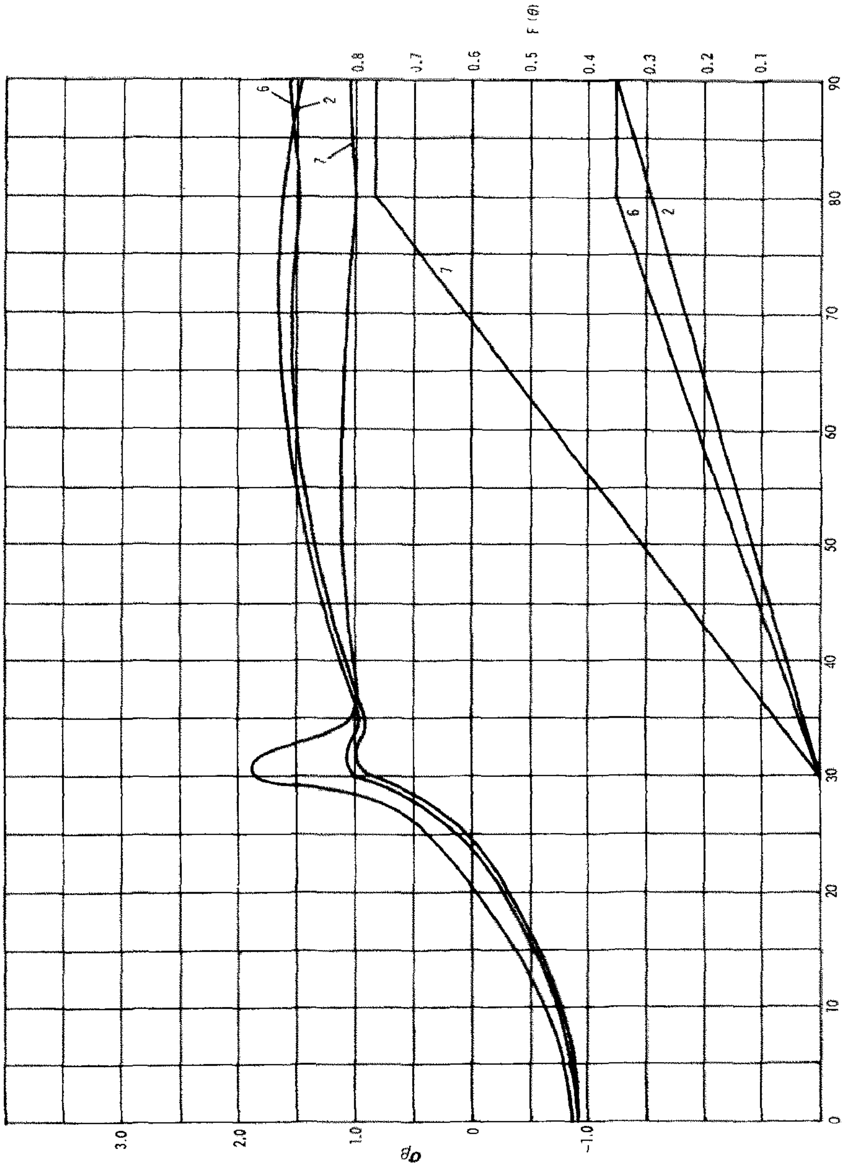

FIG. 5. σ_β and $F(\vartheta)$ as functions of ϑ, case 2, 6 and 7.

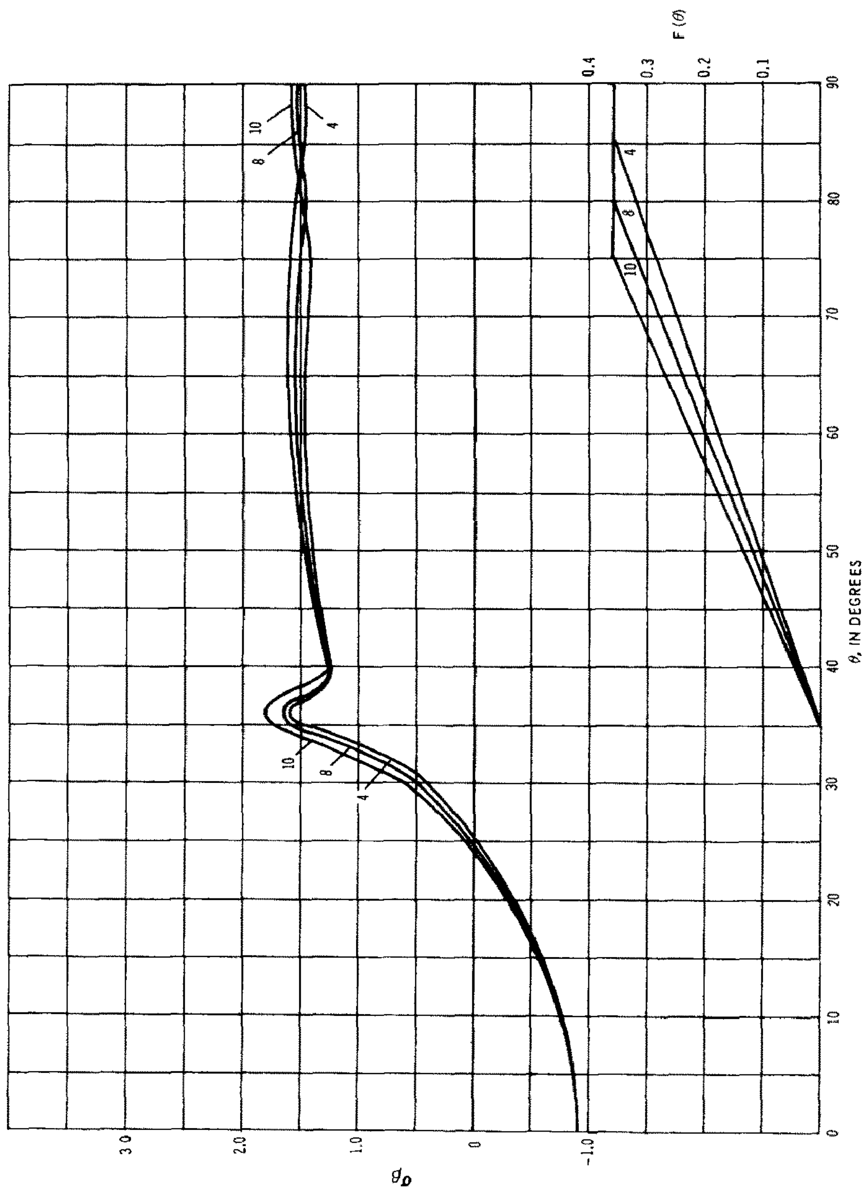

FIG. 6. σ_ϑ and $F(\vartheta)$ as functions of ϑ, case 4, 8 and 10.

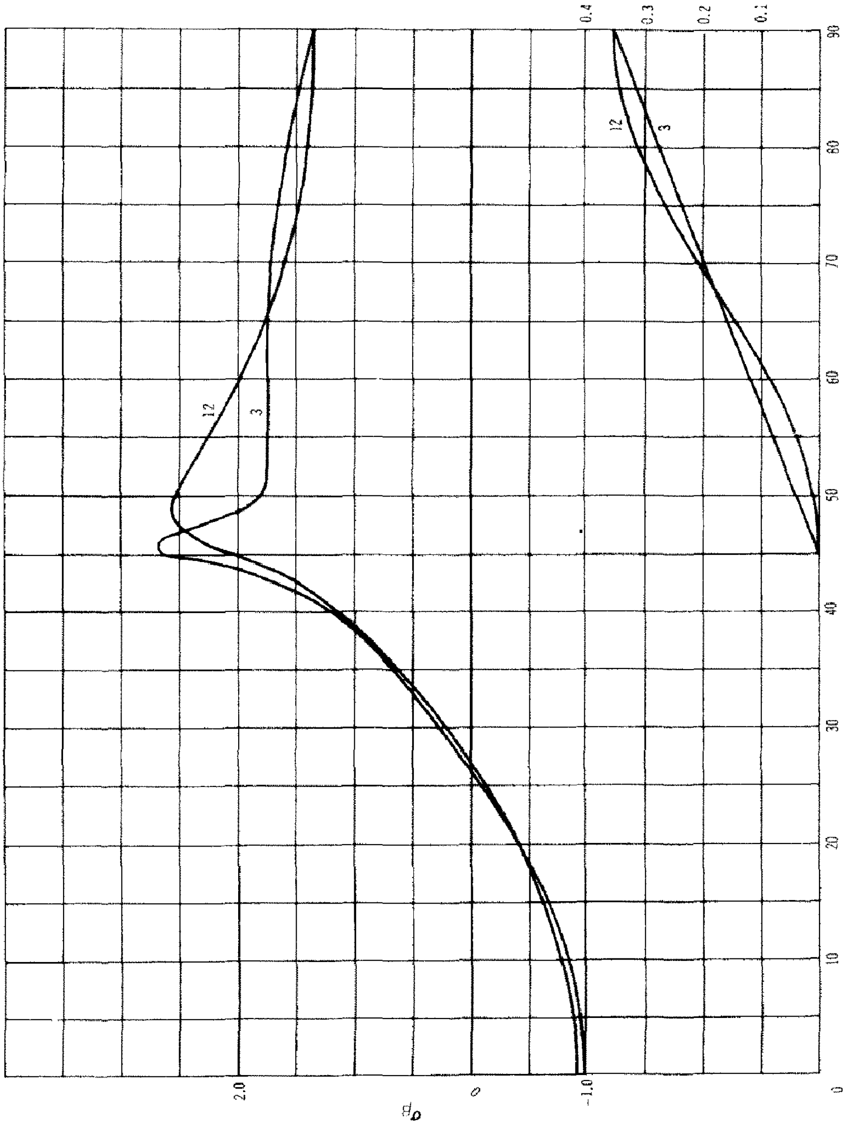

Fig. 7. σ_β and $F(\vartheta)$ as functions of ϑ, case 3 and 12

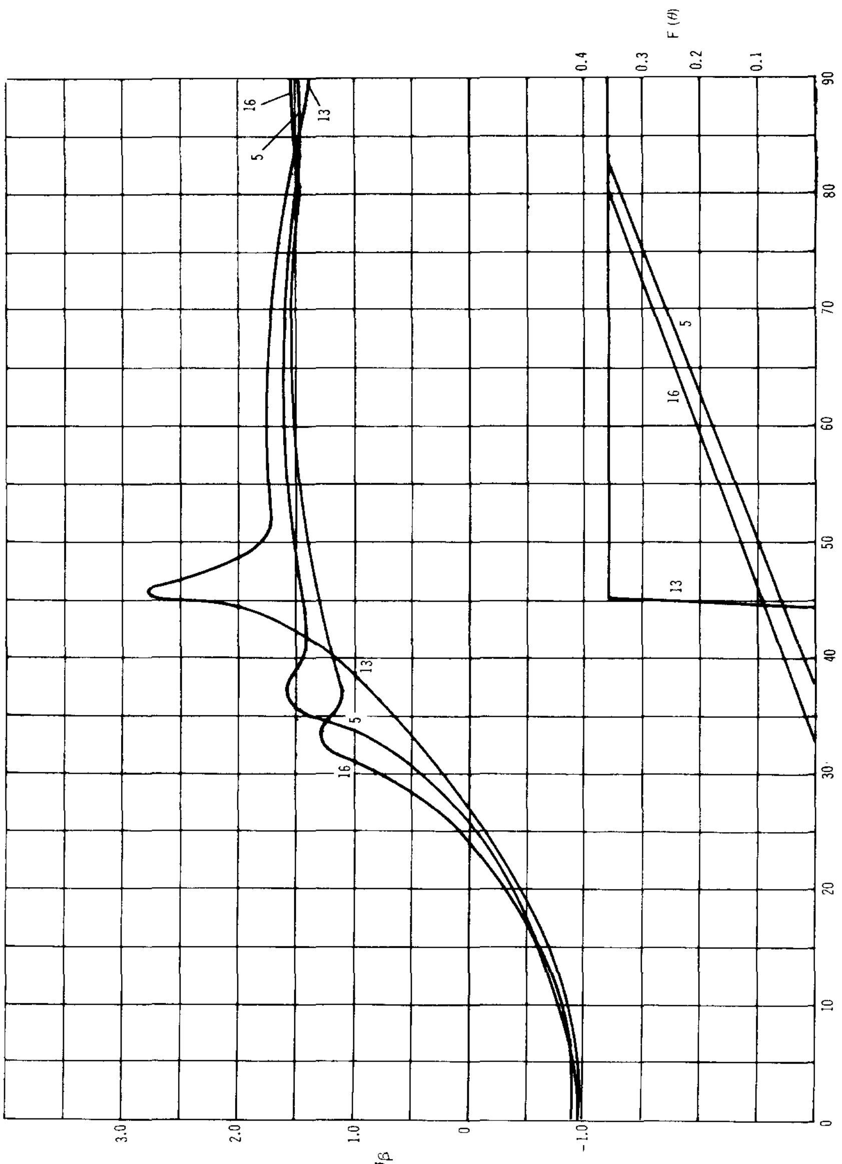

FIG. 8. σ_β and $F(\vartheta)$ as functions of ϑ, case 5, 13 and 16.

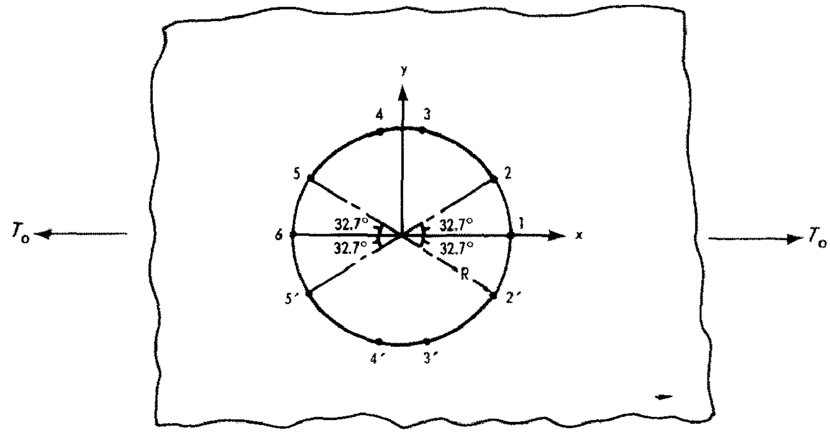

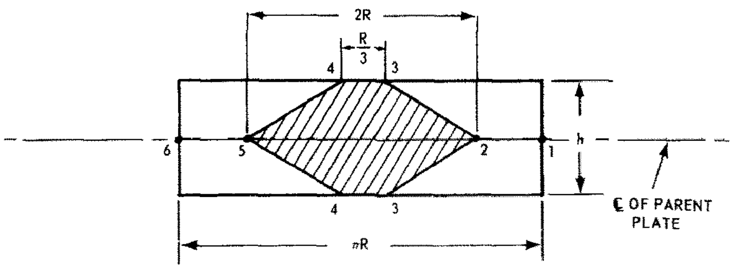

FIG. 9. Reinforcement of case 16.

shown to be approximately 63 per cent, which is substantial. As a fringe benefit the maximum stress also comes down from 1·702 (case 14) to 1·558 which amounts to about 9 per cent reduction. From a technological standpoint welding between the points 1 2 and 5 6 will also be saved which is approximately 36 per cent. The maximum value of the ratio R_e of area of reinforcement (area replaced) to area removed, as given by equation (13) can also be represented by

$$R_e = \left(\frac{h}{t} - 1\right)\frac{T}{R} \tag{21}$$

where T is the thickness of the reinforcing material. Assuming $R_e = 0{\cdot}4$ and $h/t = 11$, which are realistic values, it easily follows that $T/R = 0{\cdot}04$ which of course agrees with the assumption of a compact reinforcement. From a constructional standpoint the above type of reinforcement with its many advantages is no more complicated than a conventional all around reinforcement.

Finally, it may be pointed out that assuming R_e to be linear is not necessary but only a simplification which does not introduce large errors.

CONCLUDING REMARKS

A general method has been deduced for a new type of reinforcement of holes in large plates. An optimum or near optimum design for the reinforcement can now be achieved by the proper distribution of the reinforcing material. As an example of this method the case of a circular hole has been investigated and the numerical results are included. In a typical case 63 per cent of the weight of the reinforcing material and 36 per cent of the welding necessary can be saved and in addition the magnitude of the maximum stress can be reduced by 9 per cent as compared to the case of all around reinforcement.

This type of reinforcement may prove to be particularly useful in weight critical structures.

Acknowledgment—The authors wish to express their sincere appreciation to the Naval Ship Engineering Center for sponsoring the research embodied in this paper.

REFERENCES

[1] G. Kirsch, Die Theorie der Elasticitaet und die Beduerfnisse der Festigkeitslehre. *Z. Verein Deutscher Ing.* **32**, 797–807 (1898).
[2] S. Timoshenko, On the stresses in a flat plate with a circular hole. *J. Franklin Inst.* **197**, (1924).
[3] C. Gurney, An analysis of the stresses in a flat plate with a reinforced circular hole under edge forces. RAE Report, R. M. 1834, pp. 663–687 (1938).
[4] L. Beskin, Strengthening of circular holes in plates under edge loads. *J. appl. Mech.* **66**, A140–A148 (1944).
[5] H. Reissner and M. Morduchow, Reinforced circular cutouts in plane sheets. NACA TN 1852 (1949).
[6] J. R. M. Radok, Problems of plane elasticity for reinforced boundaries. *J. appl. Mech.* **77**, 249–254 (1955).
[7] W. H. Wittrick, Stresses around reinforced elliptical holes with application to pressure cabin windows. *Aeronaut. Q.* **X**, (1959).
[8] N. I. Muskhelishvili, *Some Basic Problems of the Mathematical Theory of Elasticity*. Noordhoff (1953).
[9] E. H. Mansfield, Neutral holes in plane sheet-reinforced holes which are elastically equivalent to the uncut sheet. *Q. J. Mech. appl. Math.* **VI**, 3 (1953).

(*Received* 10 *February* 1969; *revised* 29 *May* 1969.)

Абстракт—Предлагается новый метод усиления отверстия в плоском диске, подверженном действию одноосного растяжения. Усиляющий материал расположен только на краю отверстия в областях значительных напряжений. В виду того, что усиление прерывное, его величина, изменяемая с другой отверстия, представдяется для расчета напряжений рядами фурье. Определяются напряжения, путем использования в виде рядов двух фуикций потенциала. Ряды можно усечь в точке, после которой никакие добавочные члены не влияют существенно на величину напряжений. Даются численные значения для случая круглого отверстия, с разными типами усиления. Оканчательно, показывается, что предлагаемый тип усиления может принести приблизительно 60–70% зкономии веса, 30–35% зкономии в сварке и вблизи 10% зкономии редукции максимального напряжения, по сравнению с обычно расположенным усилением вокруг всего отверстия.